



Quantification of the influence of the C, Cr and P contents on the permeability of hydrogen through Fe alloys

I. Peñalva^{a,*}, N. Alegría^a, F. Legarda^a, C.J. Ortiz^b, R. Vila^b

^a University of the Basque Country (UPV/EHU), Energy Engineering Department, Faculty of Engineering, Plaza Ingeniero Torres Quevedo, 1, 48013 Bilbao, Spain

^b CIEMAT, Avda. Complutense 40, 28040, Madrid, Spain

ARTICLE INFO

Keywords:
Permeability
Hydrogen
Tritium
Iron Alloy

ABSTRACT

Ferritic-martensitic steels are candidate materials for blanket structural components of future thermonuclear fusion reactors. However, the tritium inventory that can be retained in different components of the reactor and its ability to migrate through the walls of any material may affect the correct operation of any fusion device. Therefore, the permeability of hydrogen isotopes through ferritic-martensitic steels, which depends on its metallurgical composition, becomes a key issue.

The European Fusion Development Agreement (EFDA) supplied 9 Fe alloys with controlled chemical alloying element contents and microstructure. The main alloying elements were C, Cr and P and they appeared in various concentrations in the 9 alloys. They were experimentally analyzed by means of the gas evolution permeation technique with temperatures ranging from 423 K to 823 K and for high purity hydrogen loading pressures ranging from 5.0×10^2 Pa to 1.5×10^5 Pa. The transport regime turned out to be diffusive and it was studied in depth, so that the permeability of each alloy was characterized by an Arrhenius-type regression for the aforementioned temperature range.

This work summarizes all the experimental measurements carried out for the permeability of hydrogen through the 9 alloys. It provides a quantification of the influence of the composition of the alloy on this transport parameter, posing different mathematical expressions for the variation of the permeability as a function of the contents of C, Cr and P.

Introduction

The properties of the ferritic-martensitic steels make this material group suitable for blanket structural components that will constitute the future thermonuclear fusion devices [1–4]. They show a good swelling resistance and a low sensitivity to helium embrittlement [5,6]. In addition, they also have favorable thermo-mechanical properties, they can withstand high neutron irradiation and temperature ranges and they have the potential for reduced or even low-neutron induced activation [7–10].

However, the limited available inventory of tritium and its uneconomic production makes its recovery one of the main goals to achieve in fusion reactors [11–13]. The operation of the reactor may be affected by the retention of tritium in different components of the reactor. On the other hand, the ability of the tritium to migrate through the walls of any material can provoke a radiological problem if it reaches rooms accessible by personnel. Therefore, the transport parameters of hydrogen

isotopes (protium, deuterium and tritium) through the materials used in fusion reactors are fundamental for its final design [14,15]. In the case of Fe alloys, these transport parameters depend on the different metallurgical components [16].

The experimental gas permeation technique was used to characterize the hydrogen permeability in 9 different Fe alloys provided by EFDA with controlled chemical alloying elements and microstructure [17]: pure Fe metal, FeC alloy, FeP alloy, FeCP alloy, Fe5Cr alloy, Fe10Cr alloy, Fe14Cr alloy, Fe10CrC alloy and Fe9CrC alloy (see Table 1). Both the chemical composition and the microstructure are significant factors for the permeability. In general, the alloys have relatively large grains. As a result, grain boundaries have most probably a very weak effect on the permeability results and, since the grain sizes are large and very similar among the alloys, the observed differences in permeability are most likely due to the chemical composition and not the microstructure. This way, although the influence of the microstructure is discussed in some points of this work, the composition has been considered as the

* Corresponding author. Tel.: +34946014277.

E-mail address: igor.penalva@ehu.eus (I. Peñalva).

<https://doi.org/10.1016/j.nme.2022.101116>

Received 25 October 2021; Received in revised form 10 December 2021; Accepted 9 January 2022

Available online 12 January 2022

2352-1791/© 2022 The Authors.

Published by Elsevier Ltd.

This is an open access article under the CC BY-NC-ND license

(<http://creativecommons.org/licenses/by-nc-nd/4.0/>).

main reason for the changes in the permeability. The results for the experimental permeability measured for most of these samples have been discussed in previous works [18–21]. In this work, all the experimental measurements carried out for the permeability of hydrogen through the 9 alloys are summarized, so that the influence of the elements on the permeation is discussed. It also provides a quantification of the influence of the composition of the alloy on this transport parameter, posing different mathematical expressions for the variation of the permeability as a function of the contents of C, Cr and P.

Material and methods

The alloys were provided as cylindrical rods of 10.9 mm diameter each, except the Fe10CrC alloy and the Fe9CrC alloy that had a diameter of 14.6 mm. A thin slice of material is required for the assembly of the permeation column. Therefore, the original cylinders were cut in small disks by CIEMAT. A cutoff machine with diamond disks was used to cut the samples to a thickness of about 1.3 mm. Then, a grinding sequence begins with 320-grit papers and then using progressively finer abrasive grits (600, 1200 and 4000) with the sample fixed in a cylinder glass with paraffin. During the polishing step, the specimens are polished with diamond paste (3 μm , 1 μm and $\frac{1}{4}$ μm) in a napped cloth. By heating at 353 K, the sample is removed from the cylinder glass before the cleaning procedure takes place: ultrasonic bath with acetone, cleaning with soap and water and final ultrasonic bath with ethanol. The sample is then dried in hot air and, once in the permeation column heated up to 823 K under ultra-high vacuum (UHV) conditions. The diameter and the final thickness of each sample that was tested, together with their mass, are shown in Table 2. The pure Fe metal is the reference material that allows the quantification of the influence of the elements on the permeability. Two different samples of this material were tested in the same facility in order to corroborate the values of the permeability that were obtained experimentally, chronologically the first and the last of the whole series with a time interval of 4 years.

The permeability of H through the samples was measured by means of the gas evolution permeation technique (see Fig. 1). The basis of this experimental technique relies on the recording of the pressure increase due to the gas flux that passes through a thin membrane of the material from a constant high gas pressure (p_h) region to a low-pressure region at initial UHV conditions. Two capacitance manometers (Baratron MKS-Instr USA), P1 and P2, measure the pressure increase with full-scale range of 1000 Pa and 13.33 Pa, respectively. Fig. 2 shows the experimental register of a typical pressure increase signal due to permeation. The mathematical analysis of the steady-state permeation flux allows the precise evaluation of the permeability under diffusion-limited regimes [22].

A thermocouple inserted into a well drilled in one of the two flanges of the permeation column measures the temperature of the sample, which is fixed by means of an electrical resistance furnace (F) regulated by a PID controller. The pressure controller (PC) is responsible for the

control of the pressure of the high-pressure face of the specimen to the desired gas driving pressure, p_h . This driving pressure is measured by means of a high-pressure transducer (HPT).

Three UHV pumping units pump down the inner volumes of the rig to the desired vacuum level. Three Penning gauges (PG) located in different zones of the facility check the vacuum state and a quadrupole mass spectrometer (QMS) is also available to check the purity of the gas and the vacuum level. Before every experimental test with high purity hydrogen (99.9999 %), UHV state is reached inside the rig (up to 10^{-7} Pa). This way, the absence of any oxygen, water vapor or any other deleterious species that may provoke surface oxidation of the specimen (S) is assured.

Theory

A diffusion-limited regime is defined when the transport of hydrogen through the material is limited by the interstitial diffusion of the gas through the bulk of the material. Under such conditions, the transport parameters that define transport of hydrogen are the diffusivity (D_{eff}), the permeability (Φ) and the Sievert's constant (K_{Seff}) that are related according to the following equation [23]:

$$K_{\text{Seff}} = \frac{\Phi}{D_{\text{eff}}} \quad (1)$$

The studied transport parameter in this work is the permeability (Φ), that relates the flux of the gas in the steady-state regime (J) through one slice of the material defined by its thickness (d), due to the pressure difference between the opposite surfaces of the slice (p_1 and p_2). Under steady-state regime, diffusion-limited flux is described by Richardson's law:

$$J = \frac{\Phi}{d} \left(p_1^{\frac{1}{2}} - p_2^{\frac{1}{2}} \right) \approx \frac{\Phi}{d} p_h^{\frac{1}{2}} \quad (2)$$

When performing an individual permeation test, these parameters are evaluated for each temperature (T) and loading pressure (p_h). The pressure increase in the low-pressure region due to the permeated flux is experimentally recorded. The theoretical expression for the pressure increase during time, $p(t)$, is obtained solving Fick's second law and gives [24,25]:

$$p(t) = \frac{RT_{\text{eff}}}{V_{\text{eff}}} \left[\frac{\Phi p_h^{1/2}}{d} A t - \frac{\Phi p_h^{1/2}}{6D_{\text{eff}}} A - \frac{2\Phi p_h^{1/2}}{\pi^2 D_{\text{eff}}} A \sum_{n=1}^{\infty} \frac{(-1)^n}{n^2} \exp\left(-D_{\text{eff}} \frac{n^2 \pi^2}{d^2} t\right) \right] \quad (3)$$

where, d is the thickness of the specimen, A the specimen area exposed to the gas volume, R is the ideal gas constant ($8.314 \text{ J K}^{-1} \text{ mol}^{-1}$), V_{eff} is the effective volume where the permeated gas is retained and T_{eff} is the temperature of the volume. The volume V_{eff} is precisely measured in each experimental permeation test by performing gas expansion to a calibrated volume.

Table 1
Chemical alloying elements and microstructure of the tested samples provided by EFDA [17].

Material	Composition [wt. ppm]						Grain size [μm]		
	C	S	O	N	P	Cr	Min	Average	Max
Fe	4	2	4	1	< 5	< 2	4	183	650
FeC	48	2	2	1	< 5	< 2	5	265	786
FeP	Centre	3	3	1	89	< 2	2	55	227
	Near the surface						2	118	475
FeCP	Centre	46	3	2	88	< 2	2	92	287
	Near the surface						2	139	374
Fe5Cr	4	3	6	2	< 5	5.40 wt%	2	68	170
Fe10Cr	4	4	4	2	< 5	10.10 wt%	3	82	259
Fe14Cr	5	7	4	5	< 10	14.25 wt%	2	141	352
Fe10CrC	820	2	2	3	< 5	10.10 wt%	Not concerned		
Fe9CrC	840	5	2	4	< 5	8.80 wt%			

Table 2

Characteristics of the samples (diameter, thickness and mass), characteristics of the tests (loading pressure and temperature ranges and total number of evaluated tests) and experimental permeability of hydrogen obtained for the tested alloys (pre-exponential permeability constant and permeation activation energy).

Material	Diameter [mm]	Thickness [mm]	Mass [g]	Loading pressure range [bar]	Temperature range [°C]	Evaluated permeation tests	Φ_0 [mol m ⁻¹ Pa ^{-0.5} s ⁻¹]	E_Φ [kJ mol ⁻¹]
Fe	A	10.9	0.57	0.01 ÷ 1.5	150 ÷ 550	40	3.90×10^{-8}	35.8
	B	10.9	0.79	0.5 ÷ 1.5	150 ÷ 550	33		
FeC	10.9	0.18	0.1226	0.005 ÷ 1.5	150 ÷ 550	39	9.18×10^{-8}	37.5
FeP	10.9	1.06	0.7645	0.1 ÷ 1.5	150 ÷ 550	38	1.68×10^{-8}	32.8
FeCP	10.9	0.97	0.6928	0.1 ÷ 1.5	150 ÷ 550	34	2.66×10^{-8}	33.9
Fe5Cr	10.9	0.88	0.5211	0.1 ÷ 1.8	150 ÷ 550	40	4.95×10^{-8}	39.7
Fe10Cr	10.9	1.30	0.8987	0.01 ÷ 1.5	150 ÷ 550	32	2.47×10^{-8}	37.8
Fe14Cr	10.9	1.30	0.7914	0.01 ÷ 1.5	200 ÷ 437	27	6.88×10^{-9}	38.8
					437 ÷ 550		6.48×10^{-4}	
Fe10CrC	14.6	1.01	1.3270	0.01 ÷ 1.5	200 ÷ 550	35	4.50×10^{-8}	40.2
Fe9CrC	14.6	1.02	1.3230	0.1 ÷ 1.5	200 ÷ 550	31	5.09×10^{-8}	39.8

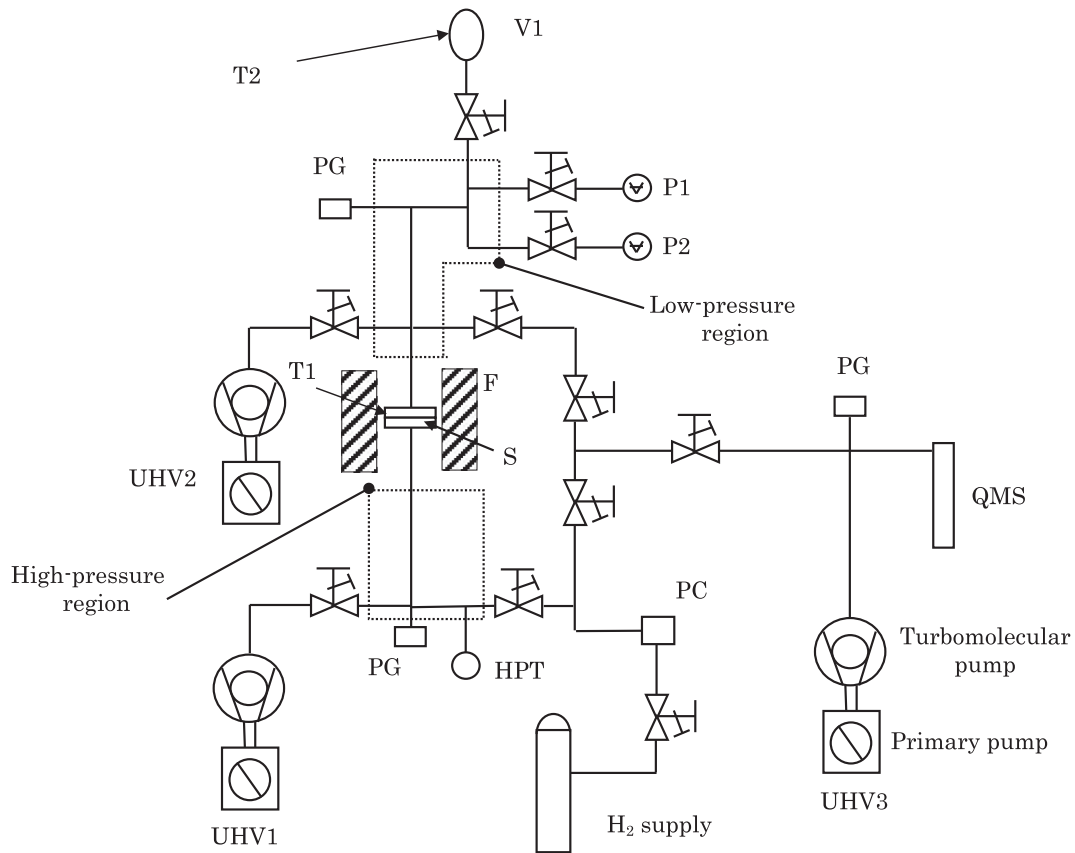


Fig. 1. Schematic view of the permeation facility. PG, Penning gauge; F, furnace; PC, pressure controller; HPT, high-pressure transducer; QMS, quadrupole mass spectrometer; S, specimen; T1, T2, thermocouples; P1, P2, capacitance manometers; UHV, ultra-high vacuum pumping units; V1, calibrated volume.

The values of the diffusivity (D_{eff}) and the permeability (Φ) for each experimental run are obtained by means of a non-linear least-squares fitting to the experimental data using Eq. (3). The Sievert's constant ($K_{\text{s, eff}}$) is then derived from the quotient of the previous transport parameters according to Eq. (1).

When considering a very large period of time ($t \rightarrow \infty$), Eq. (4) shows the evolution of pressure with time for the steady-state permeation regime:

$$p(t) = \frac{RT_{\text{eff}}}{V_{\text{eff}}} \left[\frac{\Phi p_{\text{h}}^{1/2}}{d} At - \frac{\Phi p_{\text{h}}^{1/2} d}{6D_{\text{eff}}} A \right] \quad (4)$$

This expression is valid for the steady-state flux and corresponds to

the linear tendency observed on the right-hand side of Fig. 2. When the straight line is extended down to cross the abscise axis in the time coordinate, a characteristic time known as time-lag is obtained:

$$\tau_{\text{L}} = \frac{d^2}{6D_{\text{eff}}} \quad (5)$$

Alternatively, the value of the permeability, Φ , can be derived from the slope of the straight line in the steady-state permeation regime (Fig. 2, Eq. (4)) and the diffusivity (D_{eff}) can be derived from the value of the time-lag (Fig. 2, Eq. (5)).

The permeability shows an Arrhenius-type dependency with the absolute temperature T :

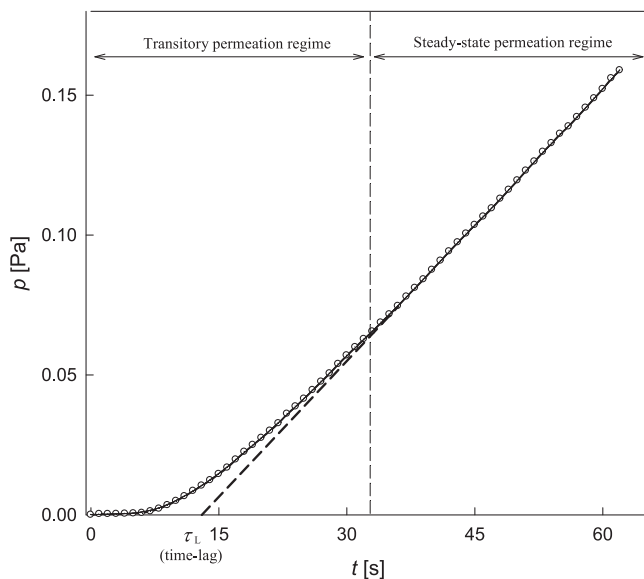


Fig. 2. Typical experimental permeation curve (FeCP, $p_h = 1.5$ bar, $T = 475$ °C): transitory permeation regime, steady-state permeation regime and definition of the time lag τ_L .

$$\Phi(T) = \Phi_0 \exp\left(\frac{-E_\phi}{RT}\right) \quad (6)$$

where Φ_0 is the pre-exponential permeability constant and E_ϕ is the permeation activation energy.

Results and discussion

A total amount of 349 individual permeation tests with 9 different materials have been taken into account in order to evaluate the influence of the composition on the permeability of hydrogen and be able to quantify the influence of the elements Cr, C and P on that transport parameter (see Table 2). The reference of material that allows that quantification has been tested twice with two different samples of the same material. The obtained values for the permeability were practically coincident for both samples and corroborate the repeatability of the measurements.

Table 2 also shows the temperature range and the loading pressure range tested for each sample. In all cases, a diffusion-limited regime was confirmed for the tested experimental ranges of loading pressures and temperatures [18–21]. This confirmation was made by means of the analysis of the proportionality of the steady-state flux to the square root of the loading pressure ($J \propto p_h^{0.5}$) according to Eq. (2), which is characteristic of diffusion-limited regime. It is important to note that the verification of the diffusion-limited regime does not imply that surface effects do not appear. In fact, the surface condition may affect significantly the processes of hydrogen permeation [26]. However, once the steady state regime is reached, the flux rate of hydrogen that permeates through the sample turns out to be limited by diffusion in the bulk of the material.

The calculation of the permeability for every permeation test (different loading pressures and temperatures in each case) was carried out by fitting the experimental curves. As expected (Eq. (6)), these values showed an Arrhenius-type dependency with temperature. Table 2 summarizes the final pre-exponential permeability constants and the permeation activation energies for permeability that allow the discussion of the influence of the contents of C, Cr and P on the permeability of hydrogen and its quantification.

Influence of the different element additions on the permeability of hydrogen

Influence of the C content

The direct way of analyzing the influence of the C content on the permeability of hydrogen is the comparison of the results for the pure Fe sample with the results for the FeC alloy. This way the possible synergetic effects caused by the presence of P or Cr are not taken into account. According to the results obtained for these two alloys (pure Fe and FeC), the permeation activation energy turns out to be similar and a slight increase of the pre-exponential permeation constant can be observed (see Table 2 and Fig. 3(a)). These data are in good agreement with data published in literature: the addition of small quantities of C in Fe alloys implies a slight increase of the permeability without affecting the permeation activation energy. When the quantity of C is increased this tendency is inverted and the permeability decreases progressively [16,27]. According to these results, the interaction of H with the bulk material seems to be slightly affected by the presence of low contents of C. This could be due to the direct interaction of H with C or with traps generated in the lattice by the addition of C to the alloy [21].

The effects caused by the presence of C can be also analyzed comparing the results of FeP versus FePC and Fe10%Cr versus Fe10%CrC, respectively (see Table 2 and Fig. 3(b) and (c)). For the alloys containing P, Fig. 3(b), a small increase of the permeation can be observed in the whole region of temperatures that were tested for the alloy containing also C. The same effect was observed when adding a similar small quantity of C to the pure Fe sample (approximately 45 ppm in weight, see Table 1). This seems to indicate that, regardless of the presence of P (in both cases approximately 88 ppm in weight, see Table 1), the addition of small quantities of C lead to a slight increase of the permeability of hydrogen [21].

In relation to the alloys containing Cr, no increase of permeability was observed when adding small quantities of C (see Fig. 3(c)). In general, the influence of the Cr content by itself seems to have a bigger influence in terms of permeability. The influence of small quantities of C seems to be negligible in the case of alloys containing Cr, as long as the values obtained for the permeability remain almost the same in these samples for the whole range of temperatures. Only a slight deviation at lowest temperatures is observed. According to these experimental results, the influence of the alloying element Cr on permeability seems to hide the effect of C [21]. However, the quantity of C added to the Fe10CrC sample is much bigger, almost 18 times bigger, than in the previous two samples (see Table 1). This bigger addition probably leads to a different behavior in the crystal lattice: small quantities of C (some tens of ppm) would dissolve in the lattice, whereas addition of bigger quantities (some hundreds of ppm) can lead to the formation of carbides [28]. These carbides would be responsible for the decrease of the permeability with increasing quantities of C, which is documented in literature [27]. Therefore, after a slight increase of the permeability due to the presence of some tens of ppm in weight of C in Fe alloys, additional increases of quantities of C would lead to smaller values of the permeability [21]. In our case, regardless of the presence of Cr, we observed a negligible effect on the permeability when adding 820 ppm in weight of C.

Influence of the Cr content

The direct way of analyzing the influence of the Cr content on the permeability of hydrogen is the comparison of the results for the pure Fe sample with the results for the Fe5Cr alloy, Fe10Cr alloy and Fe14Cr alloy. This way the possible synergetic effects caused by the presence of P or C are not taken into account, as long as the only variable content of these alloys is the one regarding Cr (see Table 1). Fig. 4(a) shows the experimental values of permeability obtained for these alloys. The permeability of the Fe5Cr alloy and the Fe10Cr alloy fit to an Arrhenius-type regression each in the whole range of temperatures that was tested. However, in the case of the Fe14Cr alloy, two Arrhenius-type regressions

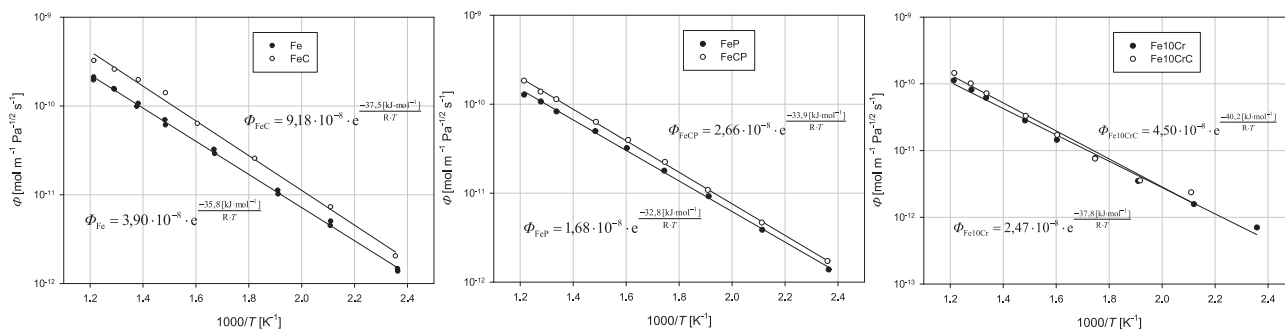


Fig. 3. Arrhenius plots of the permeability of hydrogen: (a) (pure Fe) vs. (FeC), (b) (FeP) vs. (FeCP) and (c) (Fe10Cr) vs. (Fe10CrC).

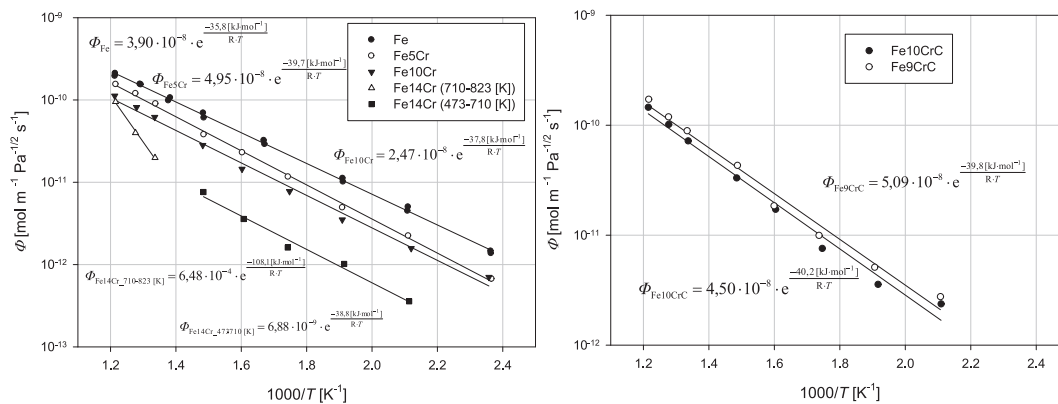


Fig. 4. Arrhenius plots of the permeability of hydrogen: (a) (pure Fe) vs. (Fe5Cr, Fe10Cr and Fe14Cr) and (b) (Fe10CrC) vs. (Fe9CrC).

were needed: one for high temperatures (above 437 °C) and a different one for low temperatures (below 437 °C) [19]. The miscibility gap reported for the Cr-Fe system [29–31] could be responsible for this need for a double fitting. The temperature and the Cr content are close to the aforementioned miscibility gap limits and, within the gap, (Cr,αFe) decomposes into (αFe) and (Cr).

In any case, the increase in the content of Cr in the alloy leads to smaller values of the permeability for the studied Cr contents in the range of temperatures and loading pressures tested experimentally [18,19]. These results are in good agreement with the general tendency described in literature [16,27]. The effect of the permeability decrease due to the increase of Cr content could be attributed to the interaction of hydrogen with the Cr atoms of the alloy that show different behaviors according to their atomic ordering. It is well-known that for low Cr concentrations, Cr atoms tend to distribute randomly in the matrix, whereas, for higher concentrations, Cr atoms tend to agglomerate into clusters [32–34]. This different behavior leads to a different microstructure. This way, depending on the Cr content of the alloy, the Cr atoms tend to the short-range ordering or to the short-range clustering [35], which makes sense with the aforementioned different behavior in terms of permeability for alloys containing more than 10% of Cr in weight. Furthermore, changes in different thermodynamic and magnetic properties have already been reported for FeCr alloys due to this behavior [36]. Besides, the lattice parameter of the bcc phases involved in FeCr alloys experiences a rapid change for small Cr concentrations [29], which may affect directly to permeability (see Fig. 4(a)). It seems reasonable to conclude that all these microstructural changes likely affect the migration of hydrogen atoms, which leads to a decreasing permeability as the Cr content increases.

Fig. 4(b) shows the experimental values of permeability obtained for the Fe10CrC alloy and the Fe9CrC alloy and the aforementioned effect of the permeability decrease when the Cr content is increased can also be observed. In this case, the influence of the presence of C seems to be

negligible as it was discussed in the previous section.

Influence of the P content

The direct way of analyzing the influence of the P content on the permeability of hydrogen is the comparison of the results for the pure Fe sample with the results for the FeP alloy. This way the possible synergistic effects caused by the presence of C or Cr are not taken into account, as long as the only variable content of these alloys is the one regarding P (see Table 1). Fig. 5(a) shows the experimental values of permeability obtained for these alloys. According to the results, the addition of P leads to a decrease in the permeability in the whole range of tested temperatures and loading pressures and the value of the permeation activation energy is also slightly smaller for the alloy containing P. When comparing the FeC alloy with the FeCP alloy, the same behavior as for the comparison of the Fe vs. FeP alloys has been observed (see Fig. 5(b)).

This effect has been already discussed [20] and might be attributed to the interstitial grain boundary segregation of P that is known as one of the most deleterious causes of intergranular embrittlement in bcc iron and ferritic steels [37,38]. The concentration of P at the grain boundaries may reach up to several tens of percent under some conditions, even though P may be involved in the alloy in quite low amounts. As a consequence, this grain boundary segregation strongly reduces the intergranular cohesion and may affect to the chemical bonding and, consequently to the permeability [39].

Analysis of the joint influences

Analysis of the joint influence of C and Cr. As discussed in the previous sections, the presence of small quantities of C in Fe alloys leads to an increase of the permeability, whereas the presence of Cr has the opposite effect [16,18,19,21,27]. According to the direct comparison of the values for the permeability of the Fe10Cr alloy and the Fe10CrC alloy (see Fig. 3 (c)), the addition of 800 ppm in weight of C does not affect to the

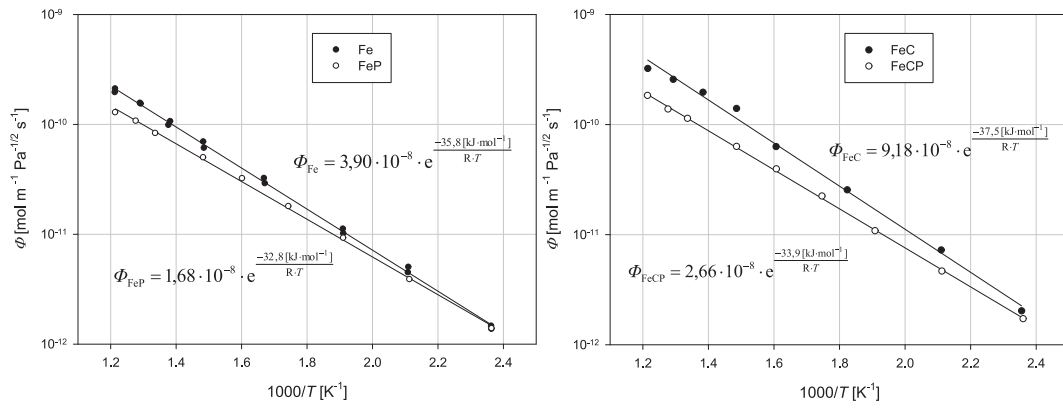


Fig. 5. Arrhenius plots of the permeability of hydrogen: (a) (pure Fe) vs. (FeP) and (b) (FeC) vs. (FeCP).

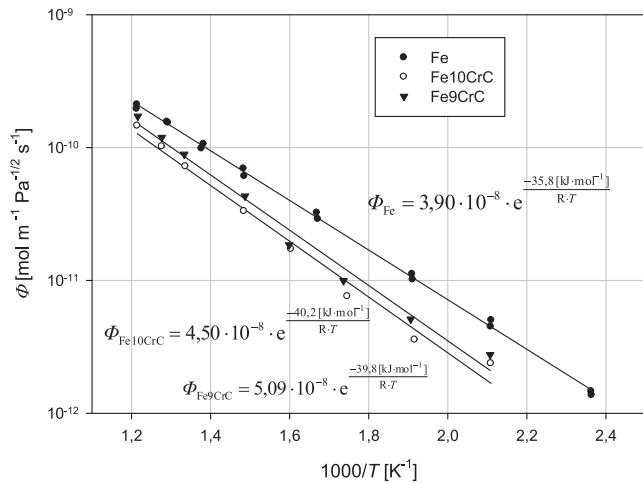


Fig. 6. Arrhenius plots of the permeability of hydrogen: (pure Fe) vs. (Fe10CrC and Fe9CrC).

permeability. In accordance with this conclusion, the Fe9CrC with similar quantities of C (see Table 1) should show a similar permeability to the sample with identical composition but without C at all. Fig. 6 depicts the values of the permeability for the pure Fe, the Fe10CrC alloy and the Fe9CrC alloy and shows that the value of the permeability for the Fe9CrC alloy is slightly bigger than the one for the Fe10CrC alloy and smaller than the one for the pure Fe. These results corroborate all the tendencies that were foreseen according to the analysis of the influence of C and Cr.

Analysis of the joint influence of C and P. As stated in the previous sections, the presence of small quantities of C in Fe alloys tends to increase the permeability. On the contrary, the presence of small quantities of P has the opposite effect [16,20,21,27]. As a result, when both elements are added in the described proportions, permeability is not significantly modified. As shown in Fig. 7, the addition of these two elements in such quantities (see Table 1) leads to values of the permeability that practically match the values of the permeability for the pure Fe sample.

It is known that the presence of C can lead to the formation of carbides that affects directly to the aforementioned grain boundary segregation [40]. In fact, in Fe-C-P alloys grain boundary segregation is affected by site competition and increasing C content on Fe alloys causes an increase of the C concentration and a decrease of the P concentration at the grain boundaries [41]. As indicated before, the average grain sizes of the tested alloys (see Table 1) could also affect to the permeability. However, since the grain sizes are large and very similar among the alloys, grain boundaries have most probably a very weak effect on the

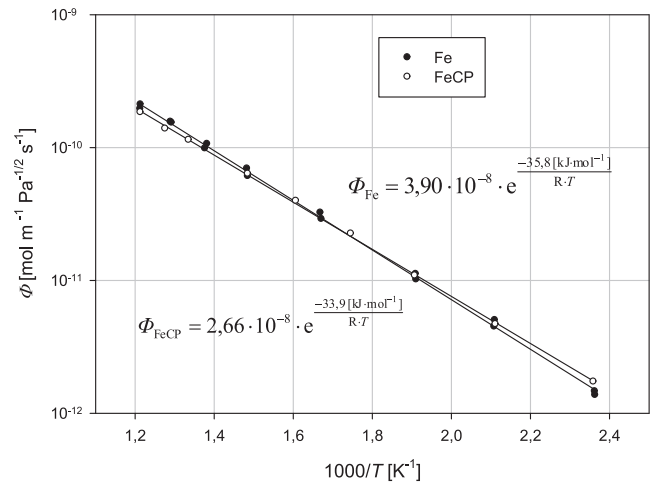


Fig. 7. Arrhenius plots of the permeability of hydrogen: (pure Fe) vs. (FeCP).

permeability results in this case. Anyway, the effects of the α -Fe grain boundaries in the segregation and clustering of H and other gases of interest in fusion is not well defined yet and it is a research task of major interest at the moment [42–45].

Global quantification of the different element additions: $\Phi = \Phi(\Phi_{Fe}, X_C, X_{Cr}, X_P)$

Taking into account the experimental results obtained for the permeability of hydrogen in the tested alloys, some mathematical expressions will be posed in order to provide a quantification of the variation of the permeability of hydrogen in Fe alloys in terms of the content of C, Cr and P. The reference permeability that will be the basis of the mathematical expressions is the one related to the pure Fe as a function of the pre-exponential permeation constant ($\Phi_{0,Fe}$) and the permeation activation energy ($E_{\phi,Fe}$):

$$\begin{aligned} \Phi_{Fe} [\text{mol m}^{-1} \text{Pa}^{-1/2} \text{s}^{-1}] &= \Phi_0 \exp\left(\frac{-E_{\phi,Fe} [\text{kJ mol}^{-1}]}{RT}\right) \\ &= 3.90 \times 10^{-8} \exp\left(\frac{-35.8 [\text{kJ mol}^{-1}]}{RT}\right) \end{aligned} \quad (7)$$

A similar study was carried out by Jung [27] based on an extensive bibliographic review of permeability values published by different research groups. However, this author did not carry out any experimental test and, as long as different techniques were used by the researchers, different mathematical expressions are provided in order to correct the corresponding pre-exponential permeation constants and

permeation activation energies as a function of the concentrations of the different elements. In this work, the mathematical expressions that will be posed will keep the mathematical formulation suggested by Jung. In addition, this work has the added value of having obtained the values of the permeability experimentally in the same facility, with the same technique, under the same test conditions and with samples where the metallurgical content is considered the only variable. In principle, according to the proposal made by Jung and as long as the composition has been considered as the main reason for the changes in the permeability, empirical relations that are posed in this work for the C, Cr and P contents can be superimposed linearly.

Quantification of the C content

The tested alloys have different contents of C (see Table 1). The FeC alloy and the FeCP alloy have approximately 50 ppm in weight and the Fe10CrC alloy and the Fe9CrC alloy approximately 800 ppm in weight. In the case of the rest of the alloys, the C content has been considered null. In line with the influence of the C content on the permeability that was discussed in the previous sections, an increase of the permeability has been verified for low contents of C (50 ppm in weight) together with a subsequent decrease as the C content increases. For the maximum content that has been tested (840 ppm in weight) the influence of C in the permeability has been considered null. These experimental results are in good agreement with the results shown by Jung [27], although this author only provides a quantification of the subsequent decrease of the permeability, taking into account Fe alloys with contents up to 2300 ppm in weight. In that study the permeation activation energies are considered constant in relation to the pure Fe alloy without any C, and the decrease of the permeability is quantified in terms of a variation of the pre-exponential permeation constant.

Taking into account the experimental measurements carried out in this work, the following mathematical expressions are posed in order to quantify the effect of the C content on the permeability of hydrogen for the temperature range that has been tested, between 150 °C and 550 °C:

- for $x_C < 0,005\%$ in weight

$$\log \frac{\Phi_{0,FeC}}{\Phi_{0,Fe}} = 74.36 x_C \quad (8)$$

$$E_{\phi,FeC} = E_{\phi,Fe} \quad (9)$$

- for 0.005% in weight $< x_C < 0.084\%$ in weight

$$\log \frac{\Phi_{0,FeC}}{\Phi_{0,Fe}} = 0.3953 - 4.70 x_C \quad (10)$$

$$E_{\phi,FeC} = E_{\phi,Fe} \quad (11)$$

where x_C is the C content expressed in % in weight; $\Phi_{0,FeC}$ is the pre-exponential permeation constant for the generic alloy with some C content and $E_{\phi,FeC}$ is the permeation activation energy for the generic alloy with some C content.

According to these expressions, the permeation activation energy remains constant for any Fe alloy that has $<0.084\%$ in weight of C. In the case of a C content of 0% in weight the permeability matches exactly the permeability of the pure Fe alloy; in the case of a C content of 0.005% in weight, the value of the pre-exponential permeation constant matches exactly the value of the pre-exponential permeation constant of the FeC alloy; and in the case of a C content of 0.084% in weight the expression matches again exactly the one that corresponds to the pure Fe.

Quantification of the Cr content

The tested alloys have different contents of Cr (see Table 1). The Fe5Cr alloy, the Fe10Cr alloy and the Fe14Cr alloy have 5.40% in

weight, 10.10% in weight and 14.25% in weight, respectively. In the case of the rest of the alloys, the Cr content has been considered null. In line with the influence of the C content on the permeability that was discussed in the previous sections, a decrease of the permeability has been verified as the Cr content is increased. According to the experimental results obtained in this work, up to a maximum content of Cr of 10.10% in weight, the appearance of Cr provokes a decrease in the permeability that can be calculated by means of a decrease of the pre-exponential permeation constant and keeping the permeation activation energy invariable. For the case of bigger contents of Cr and up to 14.25% in weight, a double Arrhenius type fitting is needed depending on the range of temperatures.

In general terms, these experimental results are in good agreement with the results shown by Jung [27]. However, this author does not distinguish different zones with different behaviors and provides only one quantification of the decrease in the permeability by changing progressively both terms simultaneously: decrease of the pre-exponential permeation constant (limited to 10% in weight for the Cr content) and increase of the permeation activation energy (limited to 13% in weight for the Cr content) as the Cr content increases.

Taking into account the experimental measurements carried out in this work, the following mathematical expressions are posed in order to quantify the effect of the Cr content on the permeability of hydrogen for the temperature range that has been tested:

- for $x_{Cr} < 10.10\%$ in weight (between 150 °C and 550 °C)

$$\log \frac{\Phi_{0,FeCr}}{\Phi_{0,Fe}} = -0.05 x_{Cr} \quad (12)$$

$$E_{\phi,FeCr} = E_{\phi,Fe} \quad (13)$$

- for 10.10% in weight $< x_{Cr} < 14.25\%$ in weight

between 200 °C and 437 °C

$$\log \frac{\Phi_{0,FeCr}}{\Phi_{0,Fe}} = -0.05 x_{Cr} \quad (14)$$

$$E_{\phi,FeCr} = E_{\phi,Fe} \quad (15)$$

between 437 °C and 550 °C

$$\log \frac{\Phi_{0,FeCr}}{\Phi_{0,Fe}} = 0.30 x_{Cr} \quad (16)$$

$$E_{\phi,FeCr} = E_{\phi,Fe} + 19.15 \sqrt{x_{Cr}} \quad (17)$$

where x_{Cr} is the Cr content expressed in % in weight; $\Phi_{0,FeCr}$ is the pre-exponential permeation constant for the generic alloy with some Cr content and $E_{\phi,FeCr}$ is the permeation activation energy for the generic alloy with some Cr content.

According to these expressions, the permeation activation energy remains constant for any Fe alloy that has $<10.10\%$ in weight of Cr and the decrease of the permeability is directly related to the decrease of the pre-exponential permeation constant according to the posed mathematical expression. In the case of a Cr content between 10.10% and 14.25% two different regions need to be distinguished as a function of the temperature. For low temperatures the previous tendency remains the same and for high temperatures the permeation activation energy also needs to be modified. The expression posed for this modification is adopted from the one posed by Jung [27], where a proportionality with the square root of the Cr content is provided.

Quantification of the P content

The tested alloys have different contents of P (see Table 1). The FeP alloy and the FeCP alloy have 89 ppm in weight and 88 ppm in weight,

respectively. In the case of the rest of the alloys, the P content has been considered null. In line with the influence of the P content on the permeability that was discussed in the previous sections, a decrease of the permeability has been verified as the P content is increased (<89 ppm in weight). These experimental results cannot be compared with the ones posed by Jung [27], as long as that author did not consider P as an element in the analysis of the influence on the permeability of hydrogen.

Taking into account the experimental measurements carried out in this work, the following mathematical expressions are posed in order to quantify the effect of the P content on the permeability of hydrogen for the temperature range that has been tested, between 150 °C and 550 °C:

- for $x_C < 0.0089\%$ in weight

$$\log \frac{\Phi_{0,FeP}}{\Phi_{0,Fe}} = -41.10 x_P \quad (18)$$

$$E_{\phi,FeP} = E_{\phi,Fe} - 337.1 x_P \quad (19)$$

where x_P is the P content expressed in % in weight; $\Phi_{0,FeP}$ is the pre-exponential permeation constant for the generic alloy with some P content and $E_{\phi,FeP}$ is the permeation activation energy for the generic alloy with some P content.

According to these expressions, in the case of a P content of 0% the permeability matches exactly the permeability of the pure Fe alloy and in the case of a P content of 0.0089%, the value of the pre-exponential permeation constant matches exactly the value of the pre-exponential permeation constant of the FeP alloy.

Conclusions

The gas permeation technique was used to study the influence of the C, Cr and P contents on the permeability of hydrogen by means of nine Fe alloys provided by EFDA with controlled chemical alloying elements and microstructure. The steady-state permeation fluxes were analyzed for every test and a diffusion-limited regime was confirmed for all the samples. The values of the permeability (ϕ) were experimentally measured for every individual test and, as a result, the permeability was calculated for each alloy by an Arrhenius-type equation in terms of the temperature.

This work summarizes all the experimental measurements carried out for the permeability of hydrogen through the 9 alloys, comprising the results of 349 individual permeation tests. The influence of the contents of the elements on the permeation of hydrogen is discussed and it provides a quantification of the influence of the composition of the alloy on this transport parameter, posing different mathematical expressions for the variation of the permeability as a function of the contents of C, Cr and P.

CRedit authorship contribution statement

I. Peñalva: Conceptualization, Methodology, Validation, Formal analysis, Investigation, Resources, Writing – original draft, Writing – review & editing, Visualization, Supervision, Project administration, Funding acquisition. **N. Alegría:** Validation, Resources, Writing – review & editing, Funding acquisition. **F. Legarda:** Validation, Resources, Writing – review & editing, Funding acquisition. **C.J. Ortiz:** Conceptualization, Validation, Writing – review & editing, Project administration. **R. Vila:** Conceptualization, Validation, Writing – review & editing, Project administration.

Declaration of Competing Interest

The authors declare that they have no known competing financial interests or personal relationships that could have appeared to influence

the work reported in this paper.

Acknowledgements

This work has been carried out in the framework of research projects funded by the Spanish Ministry of Science and Innovation (MEC08/98), the University of the Basque Country (UPV/EHU-EHU08-34) and the European Fusion Development Agreement (EFDA MAT-REMEV). The authors would also like to thank the FEMaS Coordinated Action project for the support in knowledge exchange among different research groups and Pilar Fernández from CIEMAT for the preparation of the tested samples.

References

- [1] G.A. Esteban, A. Perujo, L.A. Sedano, B. Mancinelli, *J. Nucl. Mater.* 282 (2000) 89–96.
- [2] George H. Neilson, *Magnetic Fusion Energy, From Experiments to Power Plants*, Woodhead Publishing Series in Energy: Number 99, 2016, ISBN: 978-0-08-100326-8.
- [3] M. Abdou, N.B. Morley, S. Smolentsev, A. Ying, S. Malang, A. Rowcliffe, M. Ulrickson, *Fusion Eng. Des.* 100 (2015) 2–43.
- [4] L.M. Giancarli, M. Abdou, D.J. Campbell, V.A. Chuyanov, M.Y. Ahn, M. Enoeda, C. Pan, Y. Poitevin, E. Rajendra Kumar, I. Ricapito, Y. Strebkov, S. Suzuki, P. C. Wong, M. Zmitko, *Fusion Eng. Des.* 87 (2012) 395–402.
- [5] E. Serra, A. Perujo, G. Benamati, *J. Nucl. Mater.* 245 (1997) 108–114.
- [6] K.S. Forcey, I. Iordanova, M. Yaneva, *J. Nucl. Mater.* 240 (1997) 118–123.
- [7] K. Ehrlich, S. Kelzenberg, H.-D. Röhrig, L. Schäfer, M. Schirra, *J. Nucl. Mater.* 212–215 (1994) 678–683.
- [8] G.A. Esteban, A. Perujo, K. Douglas, L.A. Sedano, *J. Nucl. Mater.* 281 (2000) 34–41.
- [9] K. Ehrlich, *Fusion Eng. Des.* 56–57 (2001) 71–82.
- [10] B. van der Schaaf, F. Tavassoli, C. Fazio, E. Rigal, E. Diegele, R. Lindau, G. LeMarois, *Fusion Eng. Des.* 69 (2003) 197–203.
- [11] E. Serra, G. Benamati, O.V. Ogorodnikova, *J. Nucl. Mater.* 255 (1998) 105–115.
- [12] G. Veredas, J. Fradera, I. Fernández, I. Peñalva, L. Mesquida, J. Abellá, J. Sempere, I. Martínez, B. Herrazti, L. Sedano, *Fusion Eng. Des.* 86 (2011) 2365–2369.
- [13] R. Sacristán, G. Veredas, I. Bonjoch, I. Peñalva, E. Calderón, G. Albarro, D. Balart, A. Sarrionandia-Ibarra, F. Legarda, *Fusion Eng. Des.* 89 (2014) 1551–1556.
- [14] R.A. Causey, *J. Nucl. Mater.* 300 (2002) 91–117.
- [15] M. Glugla, R. Lässer, L. Dörr, D.K. Murdoch, R. Haange, H. Yoshida, *Fusion Eng. Des.* 69 (2003) 39–43.
- [16] A. D. Le Claire, Report AERE-R-10598 (1982).
- [17] J. Le Coze, 2007, Procurement of Pure Fe Metal And Fe-Based Alloys with Controlled Chemical Alloying Element Contents and Microstructure, Final Report on Model Alloy Preparation, Armines Ecole Nationale Supérieure des Mines, Saint Etienne, France.
- [18] I. Peñalva, G. Albarro, J. Aranburu, F. Legarda, J. Sancho, R. Vila, C.J. Ortiz, *J. Nucl. Mater.* 442 (2013) S719–S722.
- [19] I. Peñalva, G. Albarro, F. Legarda, R. Vila, C.J. Ortiz, *Fusion Eng. Des.* 89 (2014) 1628–1632.
- [20] I. Peñalva, G. Albarro, F. Legarda, C.J. Ortiz, R. Vila, *Fusion Eng. Des.* 98–99 (2015) 2058–2062.
- [21] I. Peñalva, G. Albarro, F. Legarda, C.J. Ortiz, R. Vila, *Nucl. Mater. Energy* 9 (2016) 306–310.
- [22] I. Peñalva, G. Albarro, F. Legarda, G.A. Esteban, B. Riccardi, Interaction of Copper Alloys with Hydrogen, in: L. Collini (Ed.), *Copper Alloys, Early Applications and Current Performance-Enhancing Processes*, InTech, Rijeka, 2012, pp. 31–48.
- [23] G.A. Esteban, G. Albarro, I. Peñalva, A. Peña, F. Legarda, B. Riccardi, *Fusion Eng. Des.* 84 (2009) 757–761.
- [24] J. Crank, *The Mathematics of Diffusion*, Clarendon Press, Oxford, 1975.
- [25] H.S. Carslaw, J.C. Jaeger, *Conduction of Heat in Solids*, 2nd edition, Clarendon Press, Oxford, 1959.
- [26] G. Alefeld, J. Völkl, *Hydrogen in Metals*, Topics in Applied Physics 28 and 29, Springer-Verlag, Berlin Heidelberg, 1978.
- [27] P. Jung, *J. Nucl. Mater.* 238 (1996) 189–197.
- [28] N.I. Medvedeva, D.C. Van Aken, J.E. Medvedeva, *Comp. Mater. Sci.* 96 (2015) 159–164.
- [29] H. Okamoto, *Phase Diagrams of Binary Iron Alloys*, Monograph Series on Alloy Phase Diagrams 9, ASM International, Ohio, 1993.
- [30] J.O. Andersson, B. Sundman, *CALPHAD* 11 (1987) 83–90.
- [31] B.J. Lee, *CALPHAD* 17 (1993) 251–268.
- [32] I. Mirebeau, M. Hennion, G. Parette, *Phys. Rev. Lett.* 53 (1984) 687.
- [33] R.M. Fischer, E.J. Dulis, K.G. Carrol, *Trans. AIME* 197 (1953) 690.
- [34] H. Kuwano, Y. Hamaguchi, *J. Nucl. Mater.* 155–157 (1988) 1071–1074.
- [35] L. Malerba, G. Bonny, A. Caro, N. Juslin, R. Pasianot, N. Sandberg, On the Thermodynamic Validation of Two-Band Model Potentials for FeCr, External Report of the Belgian Nuclear Research Centre, SCKCEN-ER-16, 2006.
- [36] P. Olsson, I.A. Abrlikosov, L. Vitos, J. Wallenius, *J. Nucl. Mater.* 321 (2003) 84–90.
- [37] E.D. Hondros, M.P. Seah, S. Hofmann, Lejcek P L, in: R.W. Cahn, H Haasen (Eds.), *Physical Metallurgy*, 4th ed., North-Holland, Amsterdam, 1996, p. 1201.
- [38] H.J. Grabke, in: *Impurities in Engineering Materials*, Marcel Dekker, New York, 1999, p. 143.

- [39] P. Lejcek, J. Pokluda, P. Sandera, H. Hornikova, M. Jenko, Surf. Sci. 606 (2012) 258–262.
- [40] R.D.K. Misra, Acta Mater. 44 (11) (1996) 4367–4373.
- [41] H. Erhart, H.J. Grabke, Met. Sci. 15 (1981) 401–408.
- [42] S. Gesari, B. Irigoyen, A. Juan, Appl. Surf. Sci. 253 (2006) 1939–1945.
- [43] B. He, W. Xiao, W. Hao, Z. Tian, J. Nucl. Mater. 441 (2013) 301–305.
- [44] B. Osman Hoch, A. Metsue, J. Bouhattate, X. Feugas, Comput. Mater. Sci. 97 (2015) 276–284.
- [45] L. Zhang, C.C. Fu, E. Hayward, G.H. Lu, J. Nucl. Mater. 459 (2015) 247–258.